https://doi.org/10.5194/hess-2021-188
Preprint. Discussion started: 15 April 2021
© Author(s) 2021. CC BY 4.0 License.

Hydrology and Earth System Sciences
Discussions

A study on the drag coefficient in wave attenuation by vegetation

Zhilin Zhang[1,2,3,4], Bensheng Huang[1,2,3], Chao Tan[1,2,3], Hui Chen[1,2,3], Xiangju Cheng[4],

[1] Guangdong Research Institute of Water Resources and Hydropower, Guangzhou, 510630, China
[2] State and Local Joint Engineering Laboratory of Estuarine and Hydraulic Technology, Guangzhou 510630, China
[3] Guangdong Provincial Science and Technology Collaborative Innovation Center for Water Safety, Guangzhou 510630, China
[4] School of Civil Engineering and Transportation, South China University of Technology, Guangzhou, 510641, China

Correspondence to: Zhilin Zhang (zhilin_zhang@outlook.com)

Abstract. Vegetation in wetlands is a large-scale nature-based resource providing a myriad of services for human beings and the environment, such as dissipating incoming wave energy and protecting coastal areas. For understanding wave height attenuation by vegetation, there are two main traditional calibration approaches to the drag effect acting on the vegetation. One of them is based on the rule that wave height decays through the vegetated area by a reciprocal function and another by an exponential function. In both functions, the local wave height reduces with distance from the beginning of the vegetation depending on a damping factor (Eqs. (1) and (4)). These damping factors α' and k' are linked to the drag coefficient C_D and measurable parameters (Eqs. (3) and (5)). So there are two methods to predict C_D that quantify the effect of vegetation. In this study, a new equation is derived that connects these two damping factors (Eq.(12)). The different relations and methods to predicting the drag coefficient C_D have been investigated by 99 laboratory experiments. Finally, different relations between C_D and relevant parameters (Re, KC, and Ur) have been analyzed. The results show that α' approximately equals k' only for fully submerged vegetation, while the new equation can be used for both emerged and submerged canopy. It appears that the methods for predicting C_D by Dean (1979) and Kobayashi et al. (1993) are consistent with the well-recognized method by Dalrymple et al. (1984) for submerged vegetated canopy. But when the vegetation emerges, only the new method based on Eq. (12) leads to almost the same results as Dalrymple et al. (1984). Hence, Eq. (12) has built a bridge between these two approaches for the wave attenuation by vegetation and has proved applicable to emergent conditions of vegetation as well.

1 Introduction

To meet the current wave prevention requirements, it is of practical to construct ecological safety barrier with wetland vegetation based on natural conditions. Vegetation in wetlands can enhance the toughness of the coast and save construction investment effectively by dissipating incoming wave energy (e.g., Reguero et al., 2018). Practice also has proved that vegetation in wetlands can provide services such as enhance coastal ecosystem and biodiversity, enhance fisheries and forestry production, increase bank stability, and promote tourism economy, whereas the vegetated area occupies floodplain resources (Schaubroeck, 2017; Keesstra, 2018). Hence, it is necessary to better understand the mechanism of wave attenuation to promote the efficiency of the nature-based solution.

https://doi.org/10.5194/hess-2021-188
Preprint. Discussion started: 15 April 2021
© Author(s) 2021. CC BY 4.0 License.

Hydrology and Earth System Sciences
Discussions

Wave attenuation by vegetation is mainly induced by the drag force provided by the vegetation acting on water motion in researches such as numerical modeling (e.g., Wu et al., 2016; Suzuki et al., 2019), laboratory experiment (e.g., Hu et al., 2014; Wu and Cox, 2015, 2016), or field study (e.g., Danielsen et al., 2005; Quartel et al., 2007). The drag force is closely related to the drag coefficient C_D which quantifies the drag or resistance of vegetation in water (Chen et al., 2018). This coefficient is one of the most uncertain parameters in the complicate interaction between the vegetated area and water because the drag effect can be fairly different on various time and space scales. The calibration method for the drag coefficient is based on the perspective of wave energy dissipation and wave height reduction which will be discussed in Section 2, while Dean (1979) and Kobayashi et al. (1993) proposed that local wave height decaying through the vegetated canopy following reciprocal function and exponential function, respectively. These two calibration functions describe local wave height with a distance from the beginning of vegetation and a factor reflecting the damping. The damping factor from the reciprocal function and exponential damping factor from the exponential function are linked to the drag coefficient C_D and measurable parameters such as water depth and density of stems. For instance, Dean (1979) proposed a method to predict C_D based on the damping factor and the model later had been developed by researchers such as Knutson et al. (1982), Dalrymple et al. (1984), and Losada et al. (2016). Overall, different equations for these damping factors had been obtained under different operating conditions. Zhang et al. (2021) has compared these two calibration approaches by these featured functions directly and yielded a connection between the damping factor and the exponential damping factor then revealed a new equation to predict the drag coefficient. This article will compare these two traditional approaches from another perspective.

Then there are two relations between the damping factor following Dean (1979) and the exponential damping factor following Kobayashi et al. (1993) from two perspectives, and they were analyzed by 99 cases from collected data and experimental observations in this study. Additionally, in normal tidal conditions and the initial stage of storm surge, vegetation in wetlands can be emerged while by storm surge, vegetation is submerged or near-submerged. Existing methods for the drag coefficient had been compared to calculate the drag coefficient considering these emergence conditions. Finally, relations between C_D and the Reynolds number (R_e), the Keuglan-Carpenter number (KC), and the Ursell number (Ur) had been studied.

2 Theoretical foundations

Typically, the drag coefficient C_D is determined from the perspective of wave energy dissipation, represented by the decay of wave height. Dean (1979) proposed one of the first models for wave attenuation by vegetation in which wave height throughout the vegetated area can be expressed as a reciprocal function:

$$K_X = H(X)/H_0 = 1/(1 + \alpha' X), \quad (1)$$

where K_X (-) is the relative wave height at a distance X (m) through the vegetation field from the beginning of vegetation, $H(X)$ (m) is the local wave height, H_0 (m) is the incident wave height, and α' (m^{-1}) is the damping factor.

https://doi.org/10.5194/hess-2021-188
Preprint. Discussion started: 15 April 2021
© Author(s) 2021. CC BY 4.0 License.

Hydrology and Earth System Sciences
Discussions

Based on empirical estimates of fluid drag forces acting on vertical, rigid cylinder, Dean (1979) found that:

$$\alpha' = C_D d N H_0 / 6\pi h, \quad (2)$$

where d (m) is the diameter of circular vegetation cylinder, h (m) is the water depth, and N (stems m^{-2}) is the average number of stems per unit area.

Then Dalrymple et al. (1984) formulated an algebraic dissipation equation practicing linear theory and conservation of wave energy where α' can be expressed as:

$$\alpha' = \frac{4}{9\pi} C_D N d_v k_w H_0 \frac{\sinh^3 k_w l_s + 3\sinh k_w l_s}{\sinh k_w h(\sinh 2k_w h + 2k_w h)}, \quad (3)$$

where d_v (m) is the vegetated area per unit height of plant normal to wave direction, k_w (rad m^{-1}) is the wave number, and l_s (m) is the submerged stem height.

On the other hand, Kobayashi et al. (1993) published that the local wave height decays exponentially through submerged artificial kelp:

$$K_X = H(X)/H_0 = \exp(-k'X), \quad (4)$$

where k' (m^{-1}) is the exponential damping factor. Based on linear wave theory and the conservation equation of energy, k' was expressed as (Kobayashi et al.,1993):

$$k' \cong \frac{1}{9\pi} C_D N d_v k_w H_0 \frac{\sinh 3k_w l_s + 9\sinh k_w l_s}{\sinh k_w h(\sinh 2k_w h + 2k_w h)}, \quad (5)$$

Comparing these relations between the (exponential) damping factor and the drag coefficient (Eqs. (3) and (5)), a relation between the damping factor α' and the exponential damping factor k' is derived:

$$\alpha'/k' \cong 1, \quad (6)$$

Recently, Zhang et al. (2021) presented a relation between α' and k' looking at these featured functions directly, based on Taylor expansion. This method firstly scaled the distance X of Eqs. (1) and (4):

$$H/H_0 = 1/(1 + \alpha' X) = 1/(1 + \alpha x) = F(x), \quad (7)$$

and

$$H/H_0 = \exp(-k'X) = \exp(-kx) = G(x), \quad (8)$$

where α ($= \alpha' L$) (-) is the scaled damping factor, L (m) is the length of vegetated area, x ($= X/L$) (-) is the scaled distance through the vegetation field, k ($= k' L$) (-) is the scaled exponential damping factor, and $F(x)$ and $G(x)$ represent functions.

Then by using the Taylor expansion, when the scaled distance x equals half, the following equations had been derived:

https://doi.org/10.5194/hess-2021-188
Preprint. Discussion started: 15 April 2021
© Author(s) 2021. CC BY 4.0 License.

Hydrology and Earth System Sciences
Discussions

$$F(x) = \frac{2}{\alpha+2} - \frac{4\alpha}{(\alpha+2)^2}(x-1/2) + \frac{8\alpha^2}{(\alpha+2)^3}(x-1/2)^2 - \frac{16\alpha^3}{(\alpha+2)^4}(x-1/2)^3 + R_1(x), \quad (9)$$

and

$$G(x) = \frac{1}{e^{k/2}} - \frac{k}{e^{k/2}}(x-1/2) + \frac{k^2}{2e^{k/2}}(x-1/2)^2 - \frac{k^3}{6e^{k/2}}(x-1/2)^3 + R_2(x), \quad (10)$$

where $R_1(x)$ and $R_2(x)$ are the residual terms. The relative magnitude of each term in Eqs. (9) and (10) has been analyzed by Zhang et al. (2021), and it has revealed that the first two terms of these equations played the most significant role. Hence, considering only these two terms in Eqs. (9) and (10), the proportionality between the two first terms yields two equations, which result in:

$$\alpha/k = 2/(2-k), \quad (11)$$

which equals:

$$\alpha'/k' = 2/(2-k'L), \quad (12)$$

Equations (6) and (12) have built a bridge between the exponential function and reciprocal function, verifying that these two are reliable and capable to describe the wave height attenuation by vegetation satisfactorily. The rule of the attenuation is then limited by two functions, which can increase the reliability of the calibration. Besides, the exponential damping factor can be obtained easily based on local wave height, therefore, calculating α' in the well documented Eq. (3) on the basis of the calibrated k' is much easier than calibrating α' directly, which needs professional numerical tools.

However, application of Eq. (6) in Eq. (12) results in $k'L \cong 0$, which is not appropriate when there is vegetation in the wetland. Hence, it is worth further studying the relation between these two damping factors to help us better understanding the drag coefficient and wave attenuation by vegetation.

In addition we study the relation between C_D and three relevant hydraulic parameters, which are also frequently used to model C_D, including: 1) the Reynolds number, Re ($= u_{\max} d_v/\nu$), where ν (=1.011×10^{-6} m^2 s^{-1}) is the kinematic viscosity of water and $u_{\max}$ ($= 2\pi H_0/2T \tanh k_w h$) is the maximum horizontal wave velocity from linear wave theory, where T (s) is the wave period; 2) the Keulegan-Carpenter number, KC ($= u_{\max} T/d_v$), representing oscillatory flow around cylinders; and 3) the Ursell number, Ur ($= \lambda^2 H_0/h^3$), characterizing the balance between wave steepness and the relative water depth, where λ (m) is the wave length. The following formula is used to study the relation between C_D and these parameters:

$$C_d = a \exp(-b\bar{X}) \quad (13)$$

where $\bar{X}$ could be R_e, KC or Ur; a and b are factors.

https://doi.org/10.5194/hess-2021-188
Preprint. Discussion started: 15 April 2021
© Author(s) 2021. CC BY 4.0 License.

Hydrology and Earth System Sciences
Discussions

3 Experimental setup and instrumentations

The experiments were conducted in a wave flume in Guangdong key laboratory of hydrodynamic research at Guangdong research institute of water resources and hydropower, China. The wave flume is 80.0 m long, 1.8 m wide, and 2.6 m deep (schematized in Fig. 1a, unit: m). The wave was generated by a wave generator at one end and absorbed at the opposite end.

The start of the vegetated area was located 52.7 m from the wave generator. The uniform canopies were constructed by putting mimic plants (Fig. 1b) in holes drilled in the bottom. These two heights of mimic plants (l_s) were 0.3 and 0.5 m and d_v of the mimics was 0.057 m considering average diameters of the stem and leaves while the height ratio of them is about 0.5 (Fig. 1b). The three lengths of the canopies (L) were 4, 5, and 6 m, and two mimic stem densities (N) were 25 and 50 stems m^{-2} (N1 and N2, see Figs. 1c and 1d). These two water levels of the flume were 0.8 and 1.0 m so the corresponding water depth of the floodplain (h) were 0.3 and 0.5 m.

The original wave heights (H_{ori}) of each designed regular wave were calibrated at 30 m from the wavemaker before these tests. In this study, seven wave gages (G1 to G7) were used to measure the wave height time series, which were placed 1 m apart from each other from the beginning of the vegetated area (Fig. 1a) and we used the measurement at G1 as the incident wave height (H_0) (Wu and Cox, 2015).

Control tests were carried out with no mimic plants to reduce the influence of flume bed and sidewalls. As list in Table 1, sixteen operating modes were conducted including various conditions. Data of each test were collected more than 200 s and each case was repeated for three times.

https://doi.org/10.5194/hess-2021-188
Preprint. Discussion started: 15 April 2021
© Author(s) 2021. CC BY 4.0 License.

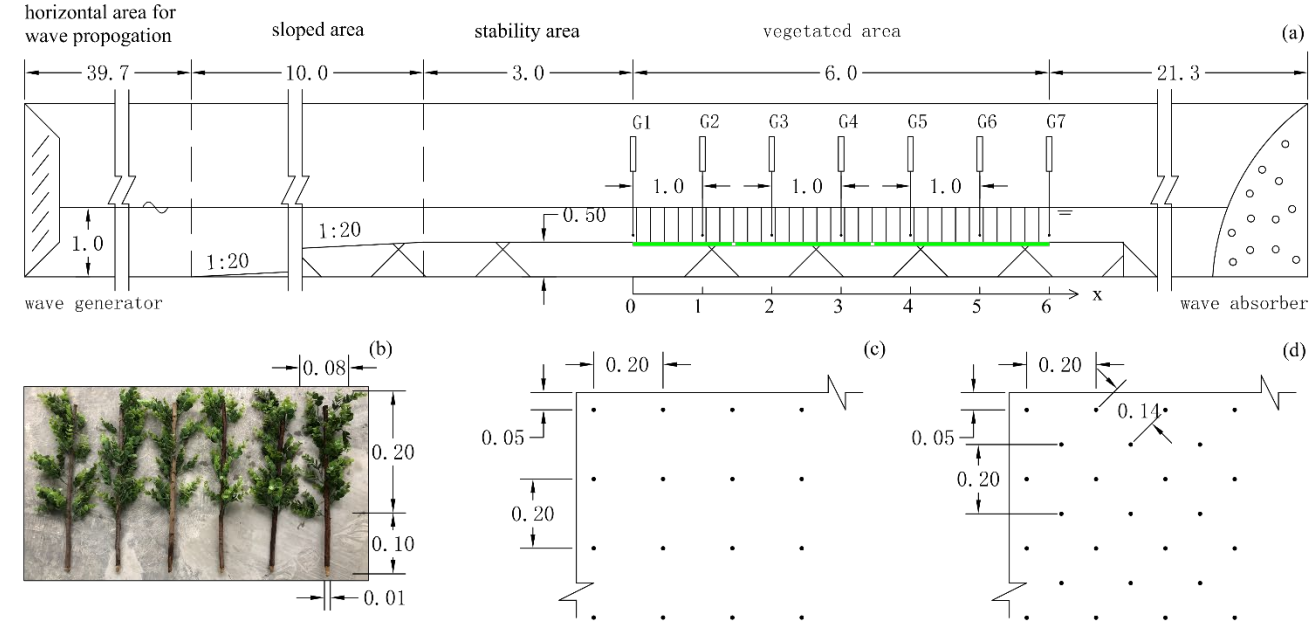

Figure 1: Experimental setup. (a) Schematic of the wave flume and instrument deployment, when the water level was 1.0 m and mimic plants height was 0.5 m; (b) mimic plants with a height of 0.3 m; (c) and (d) top view of the mimic plant canopy with density of 25 and 50 stems m^{-2}.

Table 1: Hydrodynamic conditions with regular waves

Cases	h [m]/H_{ori} [m]	k_w [-]	wave period (T) [s]	L [m]	N [stems m^{-2}]	l_s [m]
1	0.3/0.12	2.24	1.00	4	25	0.3
2	0.3/0.12	2.24	1.00	5	25	0.3
3	0.3/0.12	2.24	1.00	6	25	0.3
4	0.3/0.12	2.24	1.00	4	25	0.5
5	0.3/0.12	2.24	1.00	5	25	0.5
6	0.3/0.12	2.24	1.00	6	25	0.5
7	0.3/0.12	2.24	1.00	4	50	0.5
8	0.3/0.12	2.24	1.00	5	50	0.5
9	0.3/0.15	2.04	1.10	4	50	0.5
10	0.3/0.15	2.04	1.10	5	50	0.5
11	0.5/0.15	1.79	1.12	4	25	0.3
12	0.5/0.15	1.79	1.12	5	25	0.3
13	0.5/0.15	1.79	1.12	6	25	0.3
14	0.5/0.15	1.79	1.12	4	25	0.5

https://doi.org/10.5194/hess-2021-188
Preprint. Discussion started: 15 April 2021
© Author(s) 2021. CC BY 4.0 License.

Hydrology and Earth System Sciences
Discussions

Cases	h [m]/H_{ori} [m]	k_w [-]	wave period (T) [s]	L [m]	N [stems m^{-2}]	l_s [m]
15	0.5/0.15	1.79	1.12	5	25	0.5
16	0.5/0.15	1.79	1.12	6	25	0.5

4 Data collection

Besides experiments in this study, observations in published literature had been collected. These researchers in previous studies had shown the values of C_D and local wave height along the vegetated area.

Hu et al. (2014) conducted laboratory experiments in a wave flume, with a 6 m long vegetation mimic canopy. The mimics were stiff wooden rods with a height of 0.36 m and a diameter of 0.01 m. Three mimic stem densities (62, 139 and 556 stems m^{-2}, represented by VD1, VD2 and VD3) were constructed and control tests with no stems were measured. Also, two water depths (0.25 and 0.50 m) were used to study the emerged and submerged conditions.

Wu et al. (2011) reported a series of experiments in laboratory with a 3.66 m long vegetation field. The rigid vegetation mimicked by 9.5 mm diameter birch dowels were studied by two stem densities (350 and 623 stems m^{-2}) and two stem heights (0.63 and 0.48 m).

The laboratory experiments by Wu and Cox (2015) were conducted in a wave flume with a water depth of 12 cm and the 1.8 m long vegetated area was modeled by plastic strips, 5 mm wide by 1 mm thick. The length of the strips was 14 cm and the density was 2 100 stems m^{-2}.

Wu and Cox (2016) also conducted experiments in a small scale wave flume, and the vegetated field is 90-cm-long by uniform stand of emergent vegetation with a stem height of 0.14 m and width of 5 mm. The stem density was 1618 stems m^{-2}, and the water depth was 0.1 m.

5 Results and discussion

5.1 Reduction of wave height

Wave height along the vegetated area is a significant index for wave attenuation by vegetation. The calibrated reductions of wave height demonstrating two examples (Cases 13 and 16) were shown in Fig. 2. It is clear that Eqs. (1) and (4) were reliable relations between the scaled distance and the relative wave height. Also, Eq. (1) with calculated α value according to Eq. (11) is appliable to fit the observations, hence Eq. (11) is useful. Results showed that the larger the value of the scaled damping factor α and the scaled exponential damping factor k, the stronger the wave attenuates.

https://doi.org/10.5194/hess-2021-188
Preprint. Discussion started: 15 April 2021
© Author(s) 2021. CC BY 4.0 License.

Hydrology and Earth System Sciences
Discussions

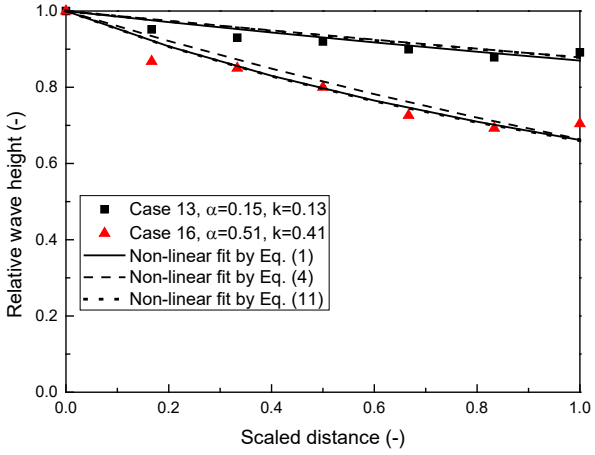

Figure 2: Measured and predicted wave attenuation. Square and trigon symbols indicated measurements of Cases 13 and 16; solid, dashed and dotted lines represented the curves fitted by Dean (1979) (Eq. (1)), Kobayashi et al. (1993) (Eq. (4)), and Eq. (11).

5.2. Relation between α and k

The relation between calibrated values of α and k by 99 cases from this study and collected data was shown in Fig. 3. In the study of Wu et al. (2011), Hu et al. (2014) and this research, both submerged and emerged cases were conducted, and in the study of Wu and Cox (2015, 2016) the vegetation canopies were emerged. The emerged and submerged canopies were separated for studying the influence of emergent condition (emerged or submerged). The results showed that there is an obvious relation between α and k. However, Eq. (6), which has been obtained by comparing these relations between the (exponential) damping factor and the drag coefficient by Dalrymple et al. (1984) and Kobayashi et al. (1993), worked well only when values of α and k were smaller than around 0.4. Equation (12), on the other hand, seemed a possible solution for the relation of these two factors, and the relation between α and k did not strongly affect by the emergent condition while these values were indeed relatively small when the vegetation was submerged ($0.04<\alpha<0.56$) than when it was emerged ($0.12<\alpha<1.43$). Notably, the analytical solution of Kobayashi et al. (1993) was obtained and conducted using deeply submerged artificial kelp, and $H(X)^3 \cong H_0 H(X)^2$ was assumed which can only be valid when wave height reduces slightly through submerged vegetated areas and the damping factors are small. This is why Eq. (6) can only be profitable for submerged vegetation.

https://doi.org/10.5194/hess-2021-188
Preprint. Discussion started: 15 April 2021
© Author(s) 2021. CC BY 4.0 License.

Hydrology and Earth System Sciences
Discussions

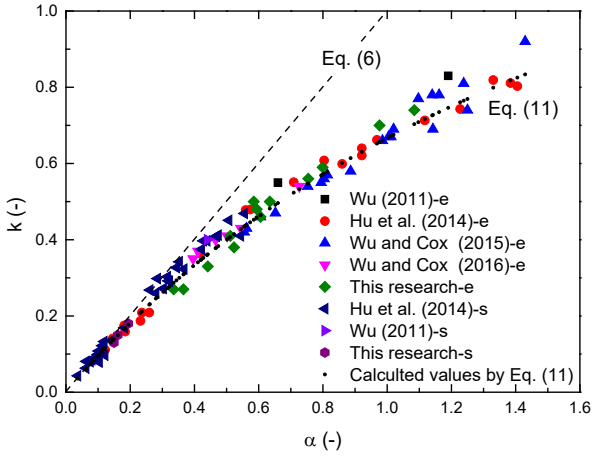

Figure 3: Comparison of calibrated α and k. Different symbols indicated cases from different researches and emergent conditions. For emerged and submerged cases, "-e" and "-s" were added after the references as the legend shown. The dashed and dotted lines indicated calculation by Eqs. (6) and (11), respectively.

5.3 Predict C_D by different methods

5.3.1 Predict C_D by Dean (1979)

Attention has been paid to study the emergent condition of the vegetation recently. This condition (eg., by l_s) has been included in Eq. (3) by Dalrymple et al. (1984) while it has not been considered in Eq. (2) by Dean (1979). In this part, the calibrated values of the drag coefficient by Eqs. (2) and (3), both considering wave height decaying by the reciprocal function, were compared. Figure 4 showed that these 99 cases obviously can be divided into two categories and they could be fitted by linear lines. The values of the adjusted R-square of the linear fit of emerged category and submerged category were 0.970 and 0.973, respectively, while the slope of the former was about twice as large as the latter. Hence, it is necessary to distinguish submerged from emerged cases when study the drag coefficient in wave attenuation by vegetation by Eq. (2). Furthermore, the linear fit of the submerged category was close to the 1:1 line which meant that both Eqs. (2) and (3) can be the solution in submerged cases but for emerged cases Eq. (2) can lead to larger values of the calibrated C_D.

https://doi.org/10.5194/hess-2021-188
Preprint. Discussion started: 15 April 2021
© Author(s) 2021. CC BY 4.0 License.

Hydrology and Earth System Sciences
Discussions
Open Access
EGU

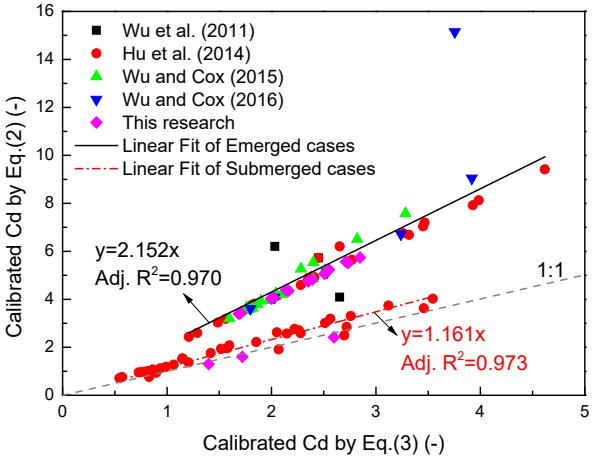

Figure 4: Comparison of the calibrated values of C_D by Eqs. (3) and (2). Different symbols indicated cases from different researches. The solid and dashed dot lines indicated linear fit of emerged and submerged categories.

5.3.2 Predict C_D by Kobayashi et al. (1993)

Equation (5) by Kobayashi et al. (1993) also considered the emergent condition and it was obtained by using local wave height decaying exponentially. Hence, in this part, the comparison of calibrated values of the drag coefficient by Eqs. (3) and (5) were studied to learn the influence of different decaying function and the result was shown in Fig. 5. The result also revealed that cases can be divided into emerged and submerged categories and the emergent condition has smaller effect on the calibrated C_D by Eq. (5) than Eq. (2). These slopes of the linear fit lines of emerged category and submerged category in Fig. 5 were 0.77 and 0.96 while the values were 2.15 and 1.16 in Fig. 4. Additionally, the linear fit line was close to the 1:1 line for submerged category hence for calculating the drag coefficient in wave attenuation by submerged vegetation, both Eqs. (3) and (5) can be the solution. This is consistent with the result in the last Section. However, for emerged cases, Eq. (5) can lead to smaller values of the calibrated C_D.

https://doi.org/10.5194/hess-2021-188
Preprint. Discussion started: 15 April 2021
© Author(s) 2021. CC BY 4.0 License.

Hydrology and Earth System Sciences
Discussions
Open Access
EGU

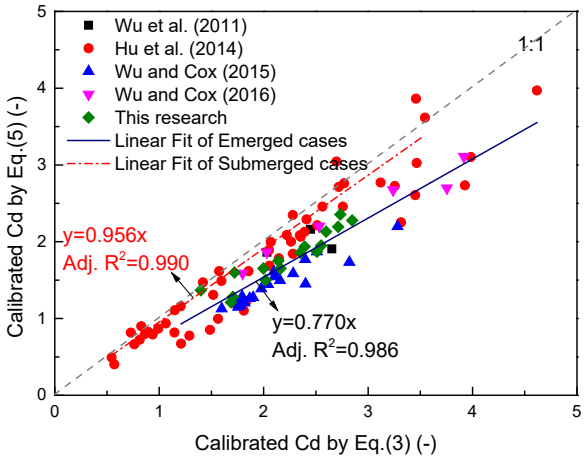

Figure 5: Comparison of the calibrated values of C_D by Eqs. (3) and (5). Details are the same as Fig. 4.

5.3.3 Predict C_D by a new method

The new method obtained the scaled damping factor α' by Eq. (12) and calculated the drag coefficient C_D by Eq. (3). The Eq. (12)-based method used the rule that the local wave height decaying exponentially and the classic relation between the damping factor and C_D by Dalrymple et al. (1984). The comparison of the calibrated values of C_D by Eq. (3) and the new method is shown in Fig. 6. The result showed that there was a strong linear relationship among the calibrated values in 99 cases from different researches. The slope of the linear fit was about unit and the adjusted R-square equalled 0.99. The result was inspiring and showed that the new method can lead to comparable results to the method by Dalrymple et al. (1984) for the drag coefficient. It is revealed that Eq. (12) is satisfactory and can be a bridge between the damping factor and the exponential damping factor and there is no need to consider the emergent condition.

https://doi.org/10.5194/hess-2021-188
Preprint. Discussion started: 15 April 2021
© Author(s) 2021. CC BY 4.0 License.

Hydrology and Earth System Sciences
Discussions
Open Access
EGU

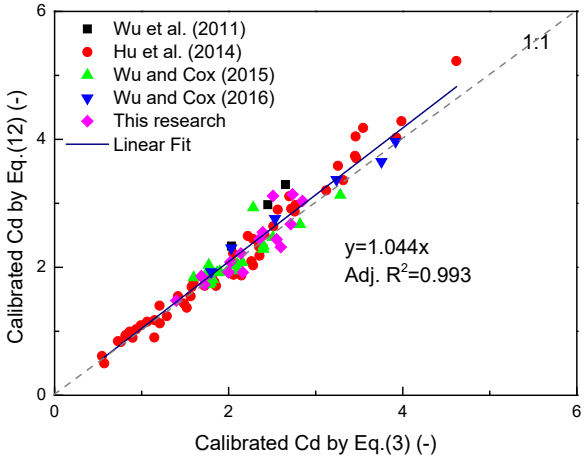

Figure 6: Comparison of the calibrated values of C_D by Eq. (3) and the new method. Different symbols indicated cases from different researches. The solid line indicated linear fit of all cases.

5.4. Relate C_D to R_e, KC, and Ur

5.4.1. Relate C_D to R_e

The relation between R_e and the calibrated C_D by the new method and the nonlinear fit by Eq. (13) were shown in Fig. 7. In the study by Hu et al. (2014) and this research, different densities were separated. These two trigons in the lower left corner of cases from Hu et al. (2014) were considered outliers in these analyses. Results showed that the tendencies of the relations were noticeable for different groups of cases as the legend specified. The values of R_e ranged from 370 to 38000, and this might due to the fact that Wu and Cox (2015, 2016) used irregular wave so the calculated Reynolds numbers were small. Results revealed that separating cases from different densities was necessary for studying this relation while the effect of the emergent condition was ignorable. Equation (13) was utilized to study the relation between R_e and C_D and the outcomes of the factors from nonlinear fit by the new method and Eq. (3) were shown in Table 2. Results showed that values for a certain factor based on the new method and Eq. (3) were close to each other especially for cases from Hu et al. (2014), supporting that the new method is comparable to Dalrymple et al. (1984). Moreover, values can be quite different in various groups hence laboratory setup could play an important role on the relation between the drag coefficient and the Reynolds number. Hence, for engineering applications, case study is needed for certain issues.

https://doi.org/10.5194/hess-2021-188
Preprint. Discussion started: 15 April 2021
© Author(s) 2021. CC BY 4.0 License.

Hydrology and Earth System Sciences
Discussions
Open Access
EGU

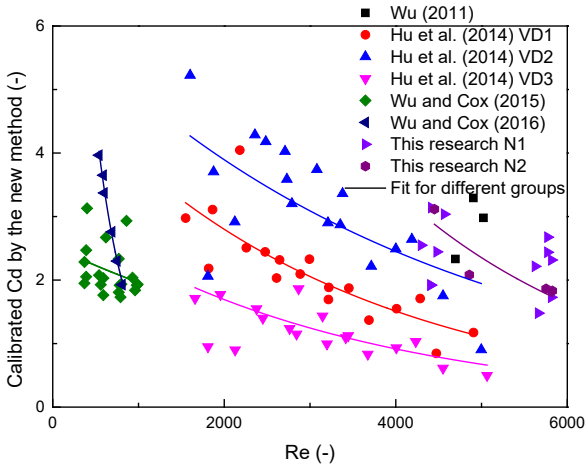

Figure 7: Relation between R_e and the calibrated C_D by the new method. Different symbols indicated cases from different researches. The solid line following the symbols indicated nonlinear fit of groups by Eq. (13).

Table 2: Outcome of the factors in Eq. (13) between R_e and C_D by the new method and Eq. (3).

References	The new method			Equation (3)		
	a	b	Adj. R^2	a	b	Adj. R^2
Hu et al. (2014) VD1	5.2	3.1×10^{-4}	0.64	4.6	2.7×10^{-4}	0.67
Hu et al. (2014) VD2	6.2	2.3×10^{-4}	0.44	5.5	2.2×10^{-4}	0.44
Hu et al. (2014) VD3	3.1	3.1×10^{-4}	0.73	3.3	3.3×10^{-4}	0.69
Wu and Cox (2015)	2.5	2.6×10^{-4}	0.04	3.0	5.4×10^{-4}	0.32
Wu and Cox (2016)	16.8	2.6×10^{-3}	0.99	/	/	/
This research N2	14.7	3.7×10^{-4}	0.69	8.3	2.8×10^{-4}	0.90

5.4.2. Relate C_D to KC

The relation between KC and the calibrated C_D was shown in Fig. 8. The values of KC ranged from 9 to 130 and the range is much smaller than that of R_e in Fig. 7. Similarly, Eqs. (13) was utilized to study the relation between KC and C_D and outcomes of the factors were shown in Table 3. Results showed that these fit lines were closer to each other than that in Fig. 7. The adjusted R-square values in Table 3 were overall larger than the corresponding numbers in Table 2. From these studied cases, the Keulegan-Carpenter number could be a satisfactory parameter for describing the drag coefficient. In addition, values for a certain factor based on these two methods were closer than the results in Table 2, revealing that the new method performed well since the method by Dalrymple et al. (1984) is well-recognized.

https://doi.org/10.5194/hess-2021-188
Preprint. Discussion started: 15 April 2021
© Author(s) 2021. CC BY 4.0 License.

Hydrology and Earth System Sciences
Discussions

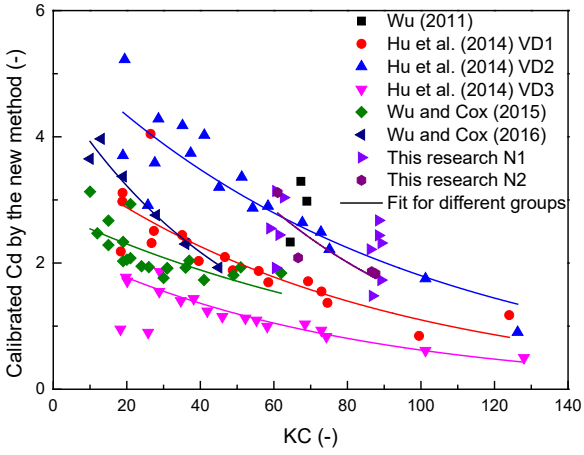

Figure 8: Relation between KC and the calibrated C_D by the new method. Details are the same as Fig. 7.

Table 3: Outcome of the factors in Eq. (13) between KC and C_D by the new method and Eq. (3).

References	The new method			Equation (3)		
	a	b	Adj. R^2	a	b	Adj. R^2
Hu et al. (2014) VD1	3.7	1.2×10^{-2}	0.67	3.4	1.1×10^{-2}	0.76
Hu et al. (2014) VD2	5.4	1.1×10^{-2}	0.76	4.8	1.0×10^{-2}	0.76
Hu et al. (2014) VD3	2.3	1.3×10^{-2}	0.94	2.4	1.5×10^{-2}	0.90
Wu and Cox (2015)	2.8	1.0×10^{-2}	0.44	3.0	1.3×10^{-2}	0.65
Wu and Cox (2016)	4.8	2.0×10^{-2}	0.94	5.0	2.4×10^{-2}	0.96
This research N2	8.0	1.7×10^{-2}	0.56	5.4	1.4×10^{-2}	0.82

5.4.3. Relate C_D to Ur

The relation between C_D and the Ursell number Ur has also been studied (Fig. 9). The values of Ur ranged from 1 to 68. However, the nonlinear fit by Eqs. (13) was unsatisfactory for all groups since the relation of these data were not strong. Results showed that comparatively, Ur was not a well-performed parameter for studying the drag coefficient in wave attenuation by vegetation.

https://doi.org/10.5194/hess-2021-188
Preprint. Discussion started: 15 April 2021
© Author(s) 2021. CC BY 4.0 License.

Hydrology and Earth System Sciences
Discussions

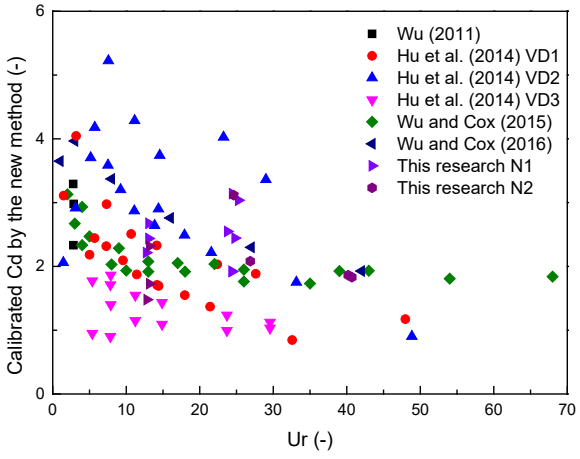

Figure 9: Relation between Ur and the calibrated C_D by the new method. Details are the same as Fig. 7.

6. Discussion and conclusions

Wave attenuation by vegetation in wetlands is a large-scale nature-based solution providing a myriad of services for human beings. For understanding wave attenuation, two main traditional calibration approaches to the drag effect acting on the vegetation were established, based on local wave height decaying by reciprocal function or exponential function. By combining these two reliable calibration methods by Dean (1979) and Kobayashi et al. (1993) from two perspectives: one by combining these featured functions directly (Eqs. (1) and (4)), and another by these relations between the (exponential) damping factor and the drag coefficient (Eqs. (3) and (5)). So, two relations between the damping factor α' and the exponential damping factor k' were derived (Eqs. (6) and (12)). Then, the relation between α' and k' and the drag coefficient in wave attenuation were analyzed by 99 laboratory experiments. Furthermore, the relation between C_D and important parameters (Re, KC, and Ur) was analysed.

The results showed that the reduction of wave height can be described by both reciprocal and exponential functions. For submerged vegetation, which reduces wave height relatively slightly, the damping factor approximately equals the exponential damping factor and Eq. (6) may be applied. However, Eq. (12) appeared applicable no matter how submerged the vegetation is, which is really a satisfactory result. These two equations build a bridge between the two traditional wave height decaying models. For submerged vegetated canopy, Eq. (2) by Dean (1979) and Eq. (5) by Kobayashi et al. (1993) were consistent with the well-recognized Eq. (3) by Dalrymple et al. (1984). However, when the vegetation was emerged, Eqs. (2) and (5) were not in line with Eq. (3). On the other hand, the predicted C_D values by the new method by Zhang et al. (2021) in combination with Eq. (3) were almost the same as those derived with the method of Dalrymple et al. (1984). Additionally, it appeared that KC

https://doi.org/10.5194/hess-2021-188
Preprint. Discussion started: 15 April 2021
© Author(s) 2021. CC BY 4.0 License.

Hydrology and Earth System Sciences
Discussions

performed best to predict C_D, better than Re and Ur, although the results can be quite different in different groups of laboratory observations. Therefore, further studies are needed in a variety of laboratory experiments.

Building a bridge between the two reliable methods by Dean (1979) and Kobayashi et al. (1993) is helpful. Firstly, it is promising that the reduction of wave height is limited by two functions so experimental outliers can be distinguished. Besides, based on local wave height, the exponential damping factor k'can be obtained easily by MS Excel, while the damping factor α'needs professional numerical tools. Therefore, calculating α' by the calibrated k' is much easier than calibrating α' directly by the well documented Eq. (3) which is the advantage of the new method in this study. This method for the drag coefficient has been validated by a great amount of data under different laboratory conditions, however, the interaction between the vegetation and flow filed is complicated so verification and/or calibration are needed further for predicting the drag coefficient.

Author contributions: Z. Zhang, B. Huang, C. Tan and H. Chen did the conceptualization and methodology. Z. Zhang and H. Chen did the data curation and formal analysis. Z. Zhang did validation and visualization. B. Huang and C. Tan did the funding acquisition and project administration. B. Huang and X. Cheng did the supervision. All the authors contributed to writing and editing of the manuscript.

Acknowledgement

The authors especially thank Dr. Hu (Zhan) and Dr. Wu (Wei-cheng) for sharing laboratory data.

Funding: This work has supported by Guangzhou Science and Technology Program key projects [grant number 201806010143]; the National Key Research and Development Program of China [grant number 2016YFC0402607].

References

Chen, H., Ni, Y., Li, Y., Feng, L., Ou, S., Su, M., Peng, Y., Hu, Z., Uijttewaal, W., and Suzuki, T.: Deriving vegetation drag coefficients in combined wave-current flows by calibration and direct measurement methods, Adv. Water Resour., 122, 217–227, https://doi.org/10.1016/j.advwatres.2018.10.008, 2018.

Dalrymple, R.A., Kirby, J.T., and Hwang, P.A.: Wave diffraction due to areas of energy dissipation, J. Waterw. Port Coast., 110(1), 67–79, https://doi.org/10.1061/(ASCE)0733-950X(1984)110:1(67), 1984.

Danielsen, F., Sørensen, M.K., Olwig, M.F, Selvam, V., Parish, F., Burgess, N.D., Hiraishi, T., Karunagaran, V.M., Rasmussen, M.S., Hansen, L.B., Quarto, A., and Suryadiputra, N.: The Asian tsunami: a protective role for coastal vegetation, Science, 310(5748), 643, https://doi.org/10.1126/science.1118387, 2005.

Dean R G.: Effects of vegetation on shoreline erosional processes. In: Wetland Functions and Values: The State of Our Understanding. Minneapolis, MN: American Water Resources Association, 415–426, 1979.

https://doi.org/10.5194/hess-2021-188
Preprint. Discussion started: 15 April 2021
© Author(s) 2021. CC BY 4.0 License.

Hydrology and Earth System Sciences
Discussions

Hu, Z., Suzuki, T., Zitman, T., Uittewaal, W., and Stive, M.: Laboratory study on wave dissipation by vegetation in combined current-wave flow, Coast. Eng., 88, 131–142, https://doi.org/10.1016/j.coastaleng.2014.02.009, 2014.

Keesstra, S., Nunes, J., Novara, A., Finger, D., Avelar, D., Kalantari, Z., and Cerdà, A.: The superior effect of nature based solutions in land management for enhancing ecosystem services, Sci. Total Environ., 610–611, 997–1009, https://doi.org/10.1016/j.scitotenv.2017.08.077, 2018.

Knutson, P.L., Brochu, R.A., Seelig, W.N., and Inskeep, M.: Wave damping in *Spartina alterniflora* marshes, Wetlands, 2, 87–104, https://doi.org/10.1007/BF03160548, 1982.

Kobayashi, N., Raichle, A.W., and Asano, T.: Wave attenuation by vegetation, J. Waterw. Port Coast., 119(1), 30–48, https://doi.org/10.1061/(ASCE)0733-950X(1993)119:1(30), 1993.

Losada, I.J., Maza, M., and Lara, J.L.: A new formulation for vegetation-induced damping under combined waves and currents, Coast. Eng., 107, 1–13, https://doi.org/10.1016/j.coastaleng.2015.09.011, 2016.

Quartel, S., Kroon, A., Augustinus, P.G.E.F., Van Santen, P.V., and Tri, N.H.: Wave attenuation in coastal mangroves in the Red River Delta, Vietnam, J Asian Earth Sci., 29(4), 576–584, https://doi.org/10.1016/j.jseaes.2006.05.008, 2007.

Reguero, B.G., Beck, M.W., Bresch, D.N., Calil, J., and Meliane, I.: Comparing the cost effectiveness of nature-based and coastal adaptation: A case study from the Gulf Coast of the United States, PLoS One, 13(4), e0192132, https://doi.org/10.1371/journal.pone.0192132, 2018.

Schaubroeck, T.: Nature-based solutions: sustainable?, Nature, 543(7645), 315, https://doi.org/10.1038/543315c, 2017.

Suzuki, T., Hu, Z., Kumada, K., Phan, L.K., and Zijlema, M.: Non-hydrostatic modeling of drag, inertia and porous effects in wave propagation over dense vegetation fields, Coast. Eng., 149, 49–64, https://doi.org/10.1016/j.coastaleng.2019.03.011, 2019.

Wu, W.M., Ozeren, Y., Wren, D.G., Chen, Q., Zhang, G., Holland, M., Ding, Y., Kuiry, S.N., Zhang, M., Jadhave, R., Chatagnier, J., Chen, Y., and Gordji, L.: Investigation of surge and wave reduction by vegetation, SERRI Report 80037-01, Southeast Region Research Initiative

Wu, W.C. and Cox, D.T.: Effects of wave steepness and relative water depth on wave attenuation by emergent vegetation, Estuar. Coast. Shelf S., 164, 443–450, https://doi.org/10.1016/j.ecss.2015.08.009, 2015.

Wu, W.C. and Cox, D.T.: Effects of vertical variation in vegetation density on wave attenuation, J. Waterw. Port Coast., 142(2), 04015020, https://doi.org/10.1061/(ASCE)WW.1943-5460.0000326, 2016.

Wu, W.C., Ma, G., and Cox, D.T.: Modeling wave attenuation induced by the vertical density variations of vegetation, Coast. Eng., 112, 17–27, https://doi.org/10.1016/j.coastaleng.2016.02.004, 2016.

Zhang, Z., Huang B., Ji, H., Tian, X., Qiu, J., Tan, C., and Cheng, X.: A rapid assessment method for calculating the drag coefficient in wave attenuation by vegetation, Acta Oceanol. Sin, 2021. (in press)